

The small x behavior of the gluon structure function from total cross sections

E.G.S. Luna^{1,2}, A.A. Natale¹ and C.M. Zanetti¹

¹*Instituto de Física Teórica, UNESP,*

São Paulo State University,

01405-900, São Paulo, SP, Brazil

²*Instituto de Física Gleb Wataghin,*

Universidade Estadual de Campinas,

13083-970, Campinas, SP, Brazil

Abstract

Within a QCD-based eikonal model with a dynamical infrared gluon mass scale we discuss how the small x behavior of the gluon distribution function at moderate Q^2 is directly related to the rise of total hadronic cross sections. In this model the rise of total cross sections is driven by gluon-gluon semihard scattering processes, where the behavior of the small x gluon distribution function exhibits the power law $xg(x, Q^2) = h(Q^2)x^{-\epsilon}$. Assuming that the Q^2 scale is proportional to the dynamical gluon mass one, we show that the values of $h(Q^2)$ obtained in this model are compatible with an earlier result based on a specific nonperturbative Pomeron model. We discuss the implications of this picture for the behavior of input valence-like gluon distributions at low resolution scales.

I. INTRODUCTION

The increase of hadronic total cross sections was theoretically predicted many years ago [1] and this prediction has been accurately verified by experiment [2]. Nowadays, one of the main theoretical tools to explain this behavior is the diffractive formalism underlying the so called QCD-inspired models [3, 4, 5, 6]. In this formalism the scattering amplitude in the c.m. system is associated with semihard processes, i.e. processes with very small x whose amplitudes can be calculated in perturbative QCD: at high energies the typical transverse momentum of semihard processes is relatively large and for wee partons in hadronic scattering processes it leads to small values for the strong coupling constant α_s . At high energies semihard processes compete with “soft” ones which have traditionally been regarded as being responsible for the bulk of the hadronic cross section. Hence the study of hadronic scattering processes is no further away from the QCD theory than, for example, the study of hard processes at small transverse distances; as the energy increases, semihard processes are expected to give an increasing and significant part of the total hadronic cross section [7, 8]. This appealing idea is a feasible one since it is well known that experimental observations made it clear that at high energies the soft and the semihard components of hadron-hadron scattering are closely related, just as, for example, the observation of correlations between the average transverse momenta of hadrons produced and the multiplicity density in rapidity, [9] and the copious production of gluon jets with moderate p_T (minijet phenomena) in hadronic collisions [10].

QCD-inspired models incorporate soft and semihard processes in the treatment of high energy hadron-hadron interactions using a diffraction-scattering formulation compatible with analyticity and unitarity constraints. At large energies and fixed transverse momentum there is a rapid growing number of semihard gluons in the hadron, which is the main reason of the rising total cross section. Therefore the rise of total hadronic cross section is intimately connected to the small x behavior of the gluon distribution function and, within the range of applicability of these models, it can be used to investigate the gluon distribution exactly in the $x \ll 1$ semihard region.

In QCD-inspired models a phenomenological gluon distribution with the behavior $g(x) \sim hx^{-J}$ is used in the actual calculations, where $J > 1$. It could be asked why this approach has not been used before to determine the small x behavior of $g(x)$. One possible reason

lies in the fact that previous models were quite dependent on an *ad hoc* infrared cutoff mass scale and on the infrared value of the strong coupling constant (α_0) [3, 4, 5]. Therefore, if $g(x)$ at small x is given by the above expression, the determination of h would not be reliable since it appears multiplied by α_0 , which is a fitting parameter in the model.

The freedom to choose the values of the mass scale and α_0 disappears in one improvement of the model, where the arbitrary mass scale is changed by a dynamical one [6]. In this model (henceforth referred to as DGM model) the onset of the dominance of semihard gluons in the interaction of high-energy hadrons is managed by the dynamical gluon mass m_g [11] (intrinsically related to an infrared finite gluon propagator, [12]) whose existence is strongly supported by recent QCD lattice simulations [13] as well as by phenomenological results [6, 11, 14, 15, 16, 17]; for recent reviews on the phenomenology of massive gluons see Ref. [18] and references therein. In the DGM model the infrared coupling constant is also a function of the dynamical gluon mass [11]. Therefore we have a precise physical meaning for this infrared coupling as well as for the quoted dynamical mass scale, which is a natural regulator of the infrared divergences associated with the semihard gluon-gluon subprocess cross sections. These properties render the DGM model instrumental for a reliable determination of the QCD-predicted small x distribution $g(x, Q^2) = h(Q^2)x^{-J}$ at moderate Q^2 , namely the determination of the $h(Q^2)$ factor, where the Q scale is on the order of the dynamical gluon mass m_g . This dynamical scale represents the onset of semihard contributions to hadronic diffractive scattering and hence provides the necessary scale in order to apply the diffractive formalism.

The gluon distribution function is usually determined in the large Q^2 region and its small x limit in this region has been extensively discussed in recent times. Therefore the results that we will discuss in this work can be considered phenomenologically important if we want to understand the match between these different kinematical regions. Moreover, the gluon distribution at a low value of $Q^2 = Q_0^2$ has to be taken into account in order to calculate the distribution at higher Q^2 via DGLAP evolution equations [19]. We show that the origin of such low Q_0^2 initial distribution can be naturally related to the phenomenon of dynamical mass generation of gluons.

The paper is organized as follows: in the next section we introduce the DGM model and show how the semihard gluon-gluon scattering can be properly eikonalized and linked to pp and $\bar{p}p$ diffractive scattering. Our results for $h(Q^2)$ at moderate Q^2 region are presented

in the Sec. III, where we also address the question of extrapolating the gluon distribution function beyond the infrared Q^2 range. In Sec. IV we draw our conclusions.

II. GLUON DISTRIBUTION AND RISING CROSS SECTIONS

In order to set a natural moderate scale Q^2 and produce a reliable determination of the factor $h(Q^2)$, we explore the small x behavior of $g(x, Q^2) = h(Q^2)x^{-J}$ in one eikonalized QCD-inspired model improved with a dynamical gluon mass [6]. This model (previously referred to as DGM model) provides a consistent calculation of total cross sections consonant with analyticity and unitarity constraints, and has already been applied successfully to describe pp and $\bar{p}p$ diffractive scattering data [6], as well as data on γp photoproduction and hadronic $\gamma\gamma$ total cross sections [17]. In the eikonal representation the total cross section is given by

$$\sigma_{tot}(s) = 4\pi \int_0^\infty b db [1 - e^{-\chi_I(b,s)} \cos \chi_R(b,s)], \quad (1)$$

where s is the square of the total center-of-mass energy, b is the impact parameter, and $\chi(b,s) = \chi_R(b,s) + i\chi_I(b,s)$ is a complex eikonal function. In the DGM model we write the even eikonal as the sum of gluon-gluon, quark-gluon, and quark-quark contributions:

$$\begin{aligned} \chi^+(b,s) &= \chi_{qq}(b,s) + \chi_{qg}(b,s) + \chi_{gg}(b,s) \\ &= i[\sigma_{qq}(s)W(b;\mu_{qq}) + \sigma_{qg}(s)W(b;\mu_{qg}) \\ &\quad + \sigma_{gg}(s)W(b;\mu_{gg})], \end{aligned} \quad (2)$$

where $\chi_{pp}^{\bar{p}p}(b,s) = \chi^+(b,s) \pm \chi^-(b,s)$. Here $W(b;\mu)$ is the overlap function in the impact parameter space and $\sigma_{ij}(s)$ are the elementary subprocess cross sections of colliding quarks and gluons ($i,j = q,g$). The overlap function is associated with the Fourier transform of a dipole form factor,

$$W(b;\mu) = \frac{\mu^2}{96\pi} (\mu b)^3 K_3(\mu b), \quad (3)$$

where $K_3(x)$ is the modified Bessel function of second kind. The odd eikonal $\chi^-(b,s)$, that accounts for the difference between pp and $\bar{p}p$ channels, is parametrized as

$$\chi^-(b,s) = C^- \Sigma \frac{m_g}{\sqrt{s}} e^{i\pi/4} W(b;\mu^-), \quad (4)$$

where m_g is the dynamical gluon mass (which will be discussed afterward) and the parameters C^- and μ^- are constants to be fitted. The factor Σ is defined as

$$\Sigma = \frac{9\pi\bar{\alpha}_s^2(0)}{m_g^2}, \quad (5)$$

with the dynamical coupling constant $\bar{\alpha}_s$ set at its frozen infrared value. The eikonal functions $\chi_{qq}(b, s)$ and $\chi_{qg}(b, s)$, needed to describe the low-energy forward data, are parametrized with terms dictated by the Regge phenomenology. The formal expressions of these quantities as well as details concerning the analyticity properties of the model amplitudes can be seen in Ref. [6].

In the DGM model the main contribution to the asymptotic behavior of hadron-hadron total cross sections comes from semihard gluon-gluon collisions. The gluon eikonal term $\chi_{gg}(b, s)$ is written as $\chi_{gg}(b, s) \equiv \sigma_{gg}(s)W(b; \mu_{gg})$, where

$$\sigma_{gg}(s) = \int_{4m_g^2/s}^1 d\tau F_{gg}(\tau) \hat{\sigma}^{DPT}(\hat{s}). \quad (6)$$

Here $F_{gg}(\tau)$ is the convoluted structure function for pair gluon-gluon ($\tau = x_1x_2$), and $\hat{\sigma}^{DPT}(\hat{s})$ is the complete cross section for the subprocess $gg \rightarrow gg$, calculated through the dynamical perturbation theory (DPT) [20], where the effective gluon propagator and coupling constant enters into the calculation. These effective quantities were obtained as solutions of the Schwinger-Dyson equations (SDE) for the gluon propagator and triple gluon vertex via the pinch technique [11], and have been used in many phenomenological calculations that are sensible to their infrared finite behavior [14, 15]. In this approach the nonperturbative running coupling $\bar{\alpha}_s$ and the functional expression of the dynamical gluon mass $M_g^2(q^2)$ are given by

$$\bar{\alpha}_s(q^2) = \frac{4\pi}{\beta_0 \ln [(q^2 + 4M_g^2(q^2))/\Lambda^2]}, \quad (7)$$

$$M_g^2(q^2) = m_g^2 \left[\frac{\ln \left(\frac{q^2 + 4m_g^2}{\Lambda^2} \right)}{\ln \left(\frac{4m_g^2}{\Lambda^2} \right)} \right]^{-12/11}, \quad (8)$$

respectively, where $\Lambda(\equiv \Lambda_{QCD})$ is the QCD scale parameter, q is the four-momentum transfer between the incoming and outgoing parton, and $\beta_0 = 11 - \frac{2}{3}n_f$ (n_f is the number of flavors). The dynamical gluon mass m_g has to be found phenomenologically, and a typical value (for

$\Lambda = 300$ MeV) is $m_g \approx 500 \pm 200$ MeV [11, 14, 15, 16, 17]. The expression of $M_g^2(q^2)$ comes out as a solution of the gluon propagator SDE and m_g is interpreted as the gluon dynamical mass, being related to the value of the propagator at $q^2 = 0$. This mass has a dynamical origin, which, in principle, should be calculated in terms of the scale Λ , and in this work it will be used as an input parameter. As discussed in detail in the Ref. [6], the total cross section $\hat{\sigma}^{DPT}(\hat{s}) = \int_{\hat{t}_{min}}^{\hat{t}_{max}} (d\hat{\sigma}/d\hat{t}) d\hat{t}$ for the subprocess $gg \rightarrow gg$ is obtained by integrating over $4m_g^2 - \hat{s} \leq \hat{t} \leq 0$. In setting these kinematical limits we have neglected the momentum behavior in Eqs. (7) and (8), since the calculation of the hadronic cross section does not depend strongly on the specific form of $M_g(q^2)$, but more on its infrared value (i.e. the value of m_g). A straightforward calculation yields

$$\hat{\sigma}^{DPT}(\hat{s}) = \frac{3\pi\bar{\alpha}_s^2}{\hat{s}} \left[\frac{12\hat{s}^4 - 55m_g^2\hat{s}^3 + 12m_g^4\hat{s}^2 + 66m_g^6\hat{s} - 8m_g^8}{4m_g^2\hat{s}[\hat{s} - m_g^2]^2} - 3 \ln \left(\frac{\hat{s} - 3m_g^2}{m_g^2} \right) \right]. \quad (9)$$

In the calculation of the structure function $F_{gg}(\tau) \equiv [g \otimes g](\tau)$ we adopt a QCD-motivated distribution functional form:

$$g(x, Q^2) = h(Q^2) \frac{(1-x)^5}{x^J}, \quad (10)$$

where the quantity $J \equiv 1 + \epsilon > 1$ controls the asymptotic behavior of $\sigma_{tot}(s)$. The factor $(1-x)^5$ is introduced in accord with the spectator counting rules at high x [21]. In the Regge language the quantity J is the intercept of the Pomeron. As we go up in energy ($s \gg \Lambda^2$ and transferred momenta $Q^2 \approx m_g^2$) the proton will be filled up with more and more semihard gluons, and we will be probing the small x region. Therefore we see that the behavior of the total hadronic cross section at higher energies is driven by only four parameters: m_g , J , h and μ_{gg} (see Eqs. (1), (2), (3) and (10)). The first two are input parameters whereas h and μ_{gg} are fitting ones. As we will see in detail in the next section, h and μ_{gg} are determined carrying out a global fit to high-energy pp and $p\bar{p}$ scattering data, namely total cross section σ_{tot} and ρ parameter data.

In the DGM model the connexion between the dynamical gluon mass m_g^2 and the scale $Q^2 \equiv -q^2$ arises as follows: the QCD improved parton model is not applicable only in the region in which the transverse momenta p_T of the colliding hadrons is of the same order as their center-of-mass energy, but also in the region in which $\sqrt{s} \gg p_T$ provided that $p_T \gg \Lambda_{QCD}$ [7, 8]. Hence it is possible to investigate the interface between high p_T region and Regge limit one by means of perturbative methods. In the DGM model we introduce the

physical energy threshold $s = 4m_g^2$ for the final state gluons (see expression (6)), assuming that these are screened gluons, in a procedure similar to the calculation of Ref. [22]. In this way, adopting the relation $p_T^2 = Q^2$, we establish the expected particle production threshold $Q = 2m_g$. Note that the gluon distribution function (10) reduces to $g(x, Q^2) = 0$ in the limit $x \rightarrow 1$, as expected by dimensional counting rules, and, more importantly, reproduces the small x QCD prediction

$$g(x, Q^2) = h(Q^2) x^{-J}. \quad (11)$$

In this context, given the high-energy nature of the data to be fitted in the following analysis, we are specially concerned with the determination of $g(x, Q)$ in its small x region and transferred momenta of the same order as the dynamical gluon masses. As we shall discuss in the next section the cross section described by Eq. (6) is totally dominated by the small x region and by processes at $Q^2 \approx 4m_g^2$. However $m_g \approx 2\Lambda_{QCD}$, as discussed in Ref. [11] (although the uncertainty in this value is of $O(\Lambda_{QCD})$), and we are in a moderate region of momenta, and above the nonperturbative region determined by the QCD scale (Λ_{QCD}).

III. THE GLUON DISTRIBUTION AT MODERATE RESOLUTION Q^2 SCALES

In the determination of the small scale dependence of the gluon distribution we explore the small x behavior of $g(x, Q)$ in one eikonalized QCD-based model improved with a dynamical gluon mass. We carry out global fits to high-energy pp and $\bar{p}p$ scattering data above $\sqrt{s} = 10$ GeV in order to determine phenomenological values for the factor h as a function of dynamical gluon mass m_g . Note that at this \sqrt{s} value the dynamics responsible for the cross section increase with energy is already effective. These data sets include the total cross section (σ_{tot}) and the ratio of the real to imaginary part of the forward scattering amplitude (ρ parameter). We use the data sets compiled and analyzed by the Particle Data Group [2], with the statistic and systematic errors added in quadrature. In all the fits we use a χ^2 fitting procedure, adopting an interval $\chi^2 - \chi_{min}^2$ corresponding, in the case of normal errors, to the projection of the χ^2 hypersurface containing 90% of probability. In the case of 8 fitting parameters (DGM model) this corresponds to the interval $\chi^2 - \chi_{min}^2 = 13.36$.

As discussed in the previous section, the behavior of the total pp and $p\bar{p}$ cross sections at higher energies is driven specially by four parameters: m_g , J , h and μ_{gg} . The input values

of the m_g have been chosen to lie in the interval $[350, 750]$ MeV, as suggested by the value $m_g = 400^{+350}_{-100}$ MeV obtained in a previous analysis of the pp and $\bar{p}p$ channels through the DGM model [6]. This input dynamical gluon mass range is also supported by recent studies via the model on survival probability of rapidity gaps in diffractive scattering [16] as well as on the γp photoproduction and the hadronic $\gamma\gamma$ total cross sections [17]. We stress that if we had used m_g as another parameter to be fitted we would reproduce the results of Fig.(1) of Ref. [6], indicating that the best gluon mass values would be in the range $[300, 750]$ MeV.

A consistent input value of J can be obtained from fitting scattering data via Regge phenomenology: in the limit of large enough s the gluon-gluon cross section $\sigma_{gg}(s)$ obtained using the gluon distribution (11) behaves as a Pomeron power law s^{J-1} :

$$\lim_{s \rightarrow \infty} \int_{4m_g^2/s}^1 d\tau F_{gg}(\tau) \hat{\sigma}^{DPT}(\hat{s}) \sim \left(\frac{s}{4m_g^2} \right)^\epsilon, \quad (12)$$

i.e. the quantity ϵ controls the asymptotic behavior of $\sigma_{gg}(s)$. We see that the asymptotic behavior of $\sigma_{gg}(s)$ in the DGM model is similar to the one expected from the Regge phenomenology, where the quantity J is related to the intercept of the Pomeron, with $J \equiv 1 + \epsilon > 1$ [23]. From fitting scattering data through an extended Regge model, the value of the Pomeron intercept J imposed by the accelerator data currently available is $J = 1.088 \pm 0.011$ [24]. This value is compatible with the recent result $J = 1.085 \pm 0.006$, obtained through the use of non-linear trajectories for the meson resonances [25]. Also, a Regge fit of the proton structure function data indicates the presence of a second Pomeron, with the hard intercept $1 + \epsilon = 1.435$ [26]. This last value of ϵ is compatible with the one expected for the exponent λ from the perturbative BFKL approach [27], namely $\lambda = \frac{12}{\pi} \alpha_s \ln 2 \approx 0.5$. However, there is a lack of theoretical precision about the precise value of λ once their value is dependent upon an infrared cut-off k_0^2 at transverse momenta of gluons [28, 29]. Moreover, it is also possible that the phenomenon of dynamical gluon mass generation push the perturbative λ value to a smaller one as was shown years ago by Ross [30]. More importantly, in what follows we will show that the use of a hard value to the Pomeron intercept gives a bad fit to σ_{tot} and ρ parameter data. It shows that in fact the increase of hadron-hadron total cross sections is governed by soft values of J , as already expected from Regge and analytical models [31, 33].

The input values for J have been extracted from the Ref. [24], where an extended Regge parametrization was used in order to establish extrema bounds for the soft Pomeron

TABLE I: Values of the input parameters and fitting ones of the DGM model resulting from the global fit to the pp and $\bar{p}p$ scattering data.

m_g [MeV]	μ_{gg} [GeV]	h	χ^2/DOF
$J = 1 + \epsilon = 1.085$			
300	0.741 \pm 0.059	0.162 \pm 0.009	1.112
350	0.782 \pm 0.064	0.226 \pm 0.013	1.111
400	0.811 \pm 0.065	0.292 \pm 0.018	1.101
450	0.857 \pm 0.073	0.357 \pm 0.021	1.114
500	0.781 \pm 0.061	0.423 \pm 0.028	1.115
550	0.878 \pm 0.072	0.525 \pm 0.037	1.107
600	0.920 \pm 0.074	0.634 \pm 0.041	1.108
650	0.909 \pm 0.071	0.708 \pm 0.052	1.107
700	0.868 \pm 0.078	0.841 \pm 0.054	1.124
750	0.956 \pm 0.078	0.993 \pm 0.065	1.124
$J = 1 + \epsilon = 1.435$			
400	0.679 \pm 0.139	0.017 \pm 0.001	1.950

intercept. In that analysis the intercept of the soft Pomeron were determined exploring the systematic uncertainty coming from the discrepancy concerning the results for $\sigma_{tot}^{\bar{p}p}$ at $\sqrt{s} = 1.8$ TeV reported by the CDF Collaboration [34] and those reported by the E710 [35] and the E811 [36] Collaborations; the values for the lower and upper bounds are $J = 1.085$ and $J = 1.095$, respectively, and represent the bounds for the soft Pomeron intercept imposed by the accelerator and cosmic ray data currently available [24]. We shall restrict ourselves to the above range of J values. Values outside this window provide bad fits to the experimental data.

The results of our global fits to the data set discussed above are depicted in Fig. 1. We note a fast increase in the h values with the dynamical gluon mass. This behavior does not depends on the specific value of the soft intercept, since the results are totally compatible for the two intercept bounds, namely $J = 1.085$ and $J = 1.095$. The χ^2/DOF values obtained in the global fits with $J = 1.085$ are relatively low, as show in Table I (the χ^2/DOF values for the input $J = 1.095$ are similar). These results (for 148 degrees of freedom) indicate

the excellence of the fits and show that it is quite unlikely that the soft Pomeron does not dominate the behavior of total cross sections at least in the energy region that we are considering. In other words, our fits do not support a hard Pomeron, as indicated in the Table I: the use of the hard input value $J = 1.435$ results in a significantly worse fit ($\chi^2/DOF = 1.95$) and shows that in this case the DGM model does not accommodate the data set used in the fitting procedure. Moreover, the input choice $J = 1.435$ results in a very low value for the factor h , namely $h = 0.017 \pm 0.001$. As we will see in the next section, this value is approximately 1/10 of the expected one [37].

The small x behavior of $xg(x, Q^2) = h(Q^2)x^{-\epsilon}$ at $Q^2 = 1 \text{ GeV}^2$, taking into account our h result for $m_g = 500 \text{ MeV}$ as indicated in Table I, is given by

$$xg(x) = (0.423 \pm 0.028)x^{-(0.085 \pm 0.05)}, \quad (13)$$

where we have adopted the intercept bound $1 + \epsilon = 1.085$ which is consistent with the recent value of J obtained from spectroscopy data analysis [25]. This behavior can be compared with the MRST result for the LO parametrization of $g(x)$ at $Q_0^2 = 1 \text{ GeV}^2$ at very small x [38]:

$$xg^{MRST}(x) \approx 3.08x^{0.10}; \quad (14)$$

at $x' = 10^{-5}$ (the kinematical limit of the MRST distributions) our distribution gives $x'g(x') = 1.125_{-0.133}^{+0.146}$, whereas $x'g^{MRST}(x') = 0.974$. This numerical agreement reinforces the assertion that the hadronic scattering is driven mainly by soft Pomerons at scales $Q^2 \lesssim 1 \text{ GeV}^2$. This is not the case for higher scales, as we can see in Figure 2, where we compare our gluon distribution with the MRST [38] and CTEQ6L1, CTEQ6L [39] leading-order gluon distributions at $Q^2 = 1.69 \text{ GeV}^2$ and $Q^2 = 4 \text{ GeV}^2$. These parton distributions are evolved with LO splitting functions using DGLAP equations from the initial scales $Q_0^2 = 1 \text{ GeV}^2$ (MRST) and $Q_0^2 = 1.69 \text{ GeV}^2$ (CTEQ6), and are obtained using tree-level formulas for the hard cross sections. The CTEQ6 (MRST) parton sets are valid in the kinematical intervals $10^{-6} \leq x \leq 1$ ($10^{-5} \leq x \leq 1$) and $1.3 \text{ GeV} \leq Q \leq 10^4 \text{ GeV}$ ($1 \text{ GeV} \leq Q \leq 10^7 \text{ GeV}$). The CTEQ6L distribution uses the same $\alpha_s(Q^2)$ coupling as the standard next-to-leading order (NLO) CTEQ fits with $\alpha_s(M_Z^2) = 0.118$ whereas CTEQ6L1 one uses the LO formula for $\alpha_s(Q^2)$ with $\Lambda_{QCD}^{4flavor} = 0.215 \text{ GeV}$ (with corresponds to $\alpha_s(M_Z^2) = 0.130$). The LO MRST distributions uses a value of $\Lambda_{QCD}^{4flavor} = 220 \text{ MeV}$ corresponding to $\alpha_s(M_Z^2) \approx 0.130$. In the

DGM model we adopt the QCD parameter value $\Lambda(n_f = 4) = 300$ MeV, which corresponds to $\bar{\alpha}_s(M_Z^2) \approx 0.130$. The results depicted in Figure 2 indicate that the small- x gluons at higher Q^2 scales are mainly generated radiatively: at the value $Q^2 = 4$ GeV² the DGM gluon distribution and the CTEQ/MRST ones are discrepant at greater than a factor of 5 at $x = 10^{-5}$, although the DGM and MRST results are compatible at $Q^2 = 1$ GeV² scale. The DGM gluon distributions at higher scales can be calculated by fitting the h results to the functional for $h(Q^2) = A + BQ^2$, as shown in Figure 3, where the best fit gives $A = 0.121 \times 10^{-1}$ and $B = 0.170 \times 10^{-5}$ MeV⁻². It is clear that the functional form of $h(Q^2)$ is not known and we stress that the choice we made above is just a guess, as well as it should be kept in mind that the Q^2 values that we are using in this function are of the order of $4m_g^2$.

It is worth mentioning that mass values $m_g \lesssim 500$ MeV are favored in other calculations of strongly interacting processes, as we will discuss later. In this way, we consider the more stringent moderate- Q^2 interval $0.36 \text{ GeV}^2 \leq Q^2 \lesssim 1 \text{ GeV}^2$ (corresponding to the gluon mass interval $300 \text{ MeV} \leq m_g \lesssim 500 \text{ MeV}$) as a more reliable one for the DGM gluon distribution. This new threshold interval for the production of dynamically generated gluons is corroborated by our results at $Q^2 \gtrsim 1.69 \text{ GeV}^2$ ($m_g \gtrsim 650 \text{ MeV}$) since our gluon distribution is smaller than the LO CTEQ6 and MRST ones. It is a clear indication that in the DGM model threshold values $m_g \gtrsim 500 \text{ MeV}$ inhibit the production of nonperturbative gluons.

At even smaller scales, for instance $Q^2 \lesssim 0.36 \text{ GeV}^2$, the x behavior of the gluon distribution is due to the dynamics of the bound state proton and is an unsolved problem of nonperturbative QCD. Hence we guess a behavior for $g(x, Q^2)$ that provides a picture more consistent with the expected behavior of the nonperturbative dynamics of the bound state nucleon [40, 41]: we assume the frozen form $g(x, \eta^2)$ for momenta $Q \leq \eta = 300$ MeV. In this way, we can write down a phenomenologically useful expression to the gluon distribution function in the range $Q \lesssim 1 \text{ GeV}$:

$$g(x, Q^2) = h(\eta^2) \frac{(1-x)^5}{x^J} \theta(\eta^2 - Q^2) + h(Q^2) \frac{(1-x)^5}{x^J} \theta(Q^2 - \eta^2). \quad (15)$$

This phenomenological gluon distribution takes into account the fact that at small Q^2 scales ($Q \lesssim 300$ MeV) the usual methods of analysis of parton distribution based on perturbative QCD are not applicable. It is clear that low- Q^2 photons do not resolve partons

in the proton and the deep inelastic scattering (DIS) formalism cannot be applied straightforwardly, and probably a generalized vector dominance model, as discussed by Alwall and Ingelman [42], is more appropriate at low Q^2 . Generally speaking we could say that we should expect a smaller gluon distribution function at moderate Q^2 than the one obtained through a strictly perturbative technique (the CTEQ approach, for instance), because of the propagator and coupling constant softening in the infrared which will appear in the cross section calculation [12, 14].

IV. CONCLUSIONS

From the diffractive formalism underlying QCD-based models we have showed how the rise of total hadronic cross sections can be naturally connected to the small x behavior of the QCD-predicted gluon distribution function $g(x, Q)$ at moderate Q^2 . We have performed a precise determination of the $h(Q^2)$ factor that appears in the QCD-predicted gluon distribution in the framework of the DGM eikonal model. This QCD-based model is instrumental for a reliable determination of the small x behavior of $g(x, Q)$ at moderate Q^2 since diffractive processes involve both semihard and soft scales resulting in a complicated interplay between perturbative and nonperturbative effects. More specifically, we have determined the behavior of the gluon distribution $g(x, Q^2) = h(Q^2)x^{-J}$ in the moderate Q interval $Q \lesssim 1$ GeV. The connexion between the resolution scale Q and the gluon dynamical mass m_g has been established by the particle production threshold $Q = 2m_g$.

Our results show that at momenta $Q^2 \gtrsim 1$ GeV² the small- x gluons are mainly generated radiatively. The coefficient h is Q^2 dependent as discussed at the end of the last section. We verified that J values like $J = 1 + \epsilon \approx 1.08$ are preferred instead of the large (hard perturbative Pomeron) value $J = 1 + \epsilon \approx 1.43$. However the rapid increase of $h(Q^2)$ with the momentum is not enough to produce a number of nonperturbative gluons as high as the perturbative ones. For this is probably necessary a rapid increase of the J values with the momentum in such a way that soft values are preferred at moderate Q^2 and hard ones would be necessary only at high Q^2 . We call attention to the fact that this statement is corroborated by a MRST group analysis of parton distributions of proton [43]. From fitting the sea quark (S) and gluon (G) distributions of the default MRST partons to the forms $xf_i(x, Q^2) = A(Q)x^{-\lambda_i(Q^2)}$ as $x \rightarrow 0$, $i = S, G$, they have look at how the exponents λ_S and

λ_G vary with Q^2 . It was observed that as Q^2 increases from the input scale $Q_0 = 1 \text{ GeV}^2$ the valence-like character of the gluon rapidly disappears due to evolution being driven by the much steeper sea. For higher values of Q^2 the gluon exponent λ_G increases rapidly and becomes higher than the sea quark exponent λ_S , since the gluon drives the sea quark via the $g \rightarrow \bar{q}q$ transition. By taking only positive values for λ_G we observe that it starts at a value where the gluon distribution is almost flat, that is $\lambda_G \approx 0$, and by $Q^2 \approx 4 \text{ GeV}^2$ it has the value $\lambda_G = 0.2$. The hard value $\lambda_G = 0.435$ is achieved at $Q^2 \approx 700 \text{ GeV}^2$. Therefore our results are consistent with the conventional view that the steeply-rising gluon component is absent at moderate Q^2 and as Q^2 increases it is generated through pQCD evolution.

The small x behavior of the gluon distribution (specifically the value of h) was performed in a different approach by Cudell, Donnachie and Landshoff (CDL) [37], within the Landshoff and Nachtmann Pomeron model (LN) [44, 45, 46]. In this model the small x gluon distribution function is given by

$$xg(x) \equiv h = \frac{4\alpha_s}{3\pi} \int dk^2 k^2 D^2(-k^2), \quad (16)$$

where the gluon propagator (D) is the effective one with the perturbative part subtracted from the integral. Notice that Eq. (16) does not contain the $x^{-\epsilon}$ contribution which has to be put by hand in the LN model. This calculation with Cornwall's propagator, where we can substitute α_s by $\bar{\alpha}_s$, gives $h \approx 0.15$: this value is basically equal to the value obtained in CDL approach [37]. A comparison of our results with the CDL one shows that our values of h are quite reasonable. More explicitly, shows that the CDL result of h is compatible with the DGM one at mass scales on the order of $m_g \approx 300 \text{ MeV}$ (see Table I). Dynamical gluon masses of that order were obtained in Ref. [16] in order to obtain the survival probability $\langle |S|^2 \rangle$ of rapidity gaps in diffractive scattering from production of Higgs boson via $WW \rightarrow H$ fusion processes. These survival factors are compatible with recent results of $\langle |S|^2 \rangle$ obtained by Khoze, Martin and Ryskin through a two-channel eikonal model which embodies pion-loop insertions in the Pomeron trajectory, diffractive dissociation, and rescattering effects [47]. In addition, in the analysis via DGM model of the γp photoproduction and the hadronic $\gamma\gamma$ total cross sections, both derived from the pp and $p\bar{p}$ scattering amplitudes assuming vector meson dominance, there is room for smaller values of m_g beside the adopted mass scale $m_g = 400 \text{ GeV}$ [17]. All these results suggest a most restrictive mass range than the one we have considered up to now. Given the behavior of $g(x, Q^2)$ obtained through the

DGM model, we can be confident in the mass range $m_g \lesssim 500$ MeV as a more reliable one. This corresponds to the Q^2 scale interval $Q^2 \lesssim 1$ GeV². It is clear that the dynamical gluon mass is a concept that has not been made totally compatible with perturbative QCD, this will probably demand time and a great effort, although the introduction of this concept is clearly consistent with the experimental data and indicate a more appealing view to the behavior of $g(x)$ at small x and moderate Q^2 .

In summary, we think that the DGM model is an useful tool in determining the behavior of the gluon distribution function at moderate Q^2 by merging in a natural way the soft and the semihard components of hadronic scattering processes. We emphasize that it is a nontrivial result that our gluon distribution behavior at small x is on the order of the MRST one at $Q^2 = 1$ GeV². This is achieved with only three parameters, namely m_g , J and h . The natural relation between the momentum scale Q and the dynamical gluon mass m_g argues the dynamical mass generation of partons to be the main mechanism behind the nonperturbative dynamics of the valence-like parton distributions present at low resolution scales.

Acknowledgments

This research was supported by the Conselho Nacional de Desenvolvimento Científico e Tecnológico-CNPq (EGSL , AAN and CMZ).

-
- [1] H. Cheng and T.T. Wu, Phys. Rev. Lett. **24**, 1456 (1970); G.V. Frolov, V.N. Gribov, and L.N. Lipatov, Phys. Lett. B **31**, 34 (1970).
 - [2] W.-M. Yao *et al.*, J. Phys. G **33**, 1 (2006).
 - [3] M.M. Block, R. Fletcher, F. Halzen, B. Margolis, and P. Valin, Nucl. Phys. B (Proc. Suppl.) **12**, 238 (1990); M.M. Block, E.M. Gregores, F. Halzen, and G. Pancheri, Phys. Rev. D **60**, 054024 (1999).
 - [4] A. Corsetti, R.M. Godbole, and G. Pancheri, Phys. Lett. B **435**, 441 (1998); G. Pancheri, R. Godbole, A. Grau, and Y.N. Srivastava, Acta Phys. Polon. B **36**, 735 (2005); R.M. Godbole, A. Grau, G. Pancheri, and Y.N. Srivastava, Phys. Rev. D **72**, 076001 (2005).

- [5] L. Durand and H. Pi, Phys. Rev. Lett. **58**, 303 (1987); Phys. Rev. D **38**, 78 (1988); *ibid.* **40**, 1436 (1989).
- [6] E.G.S. Luna *et al.*, Phys. Rev. D **72**, 034019 (2005).
- [7] L.V. Gribov, E.M. Levin, and M.G. Ryskin, Phys. Rep. **100**, 1 (1983).
- [8] E.M. Levin and M.G. Ryskin, Phys. Rep. **189**, 267 (1990).
- [9] G. Arnison *et al.*, Phys. Lett. B **118**, 167 (1982).
- [10] G. Arnison *et al.*, Phys. Lett. B **123**, 115 (1983).
- [11] J.M. Cornwall, Phys. Rev. D **26**, 1453 (1982); J.M. Cornwall and J. Papavassiliou, Phys. Rev. D **40**, 3474 (1989); J. Papavassiliou and J.M. Cornwall, Phys. Rev. D **44**, 1285 (1991); A.C. Aguilar and J. Papavassiliou, JHEP **0612**, 012 (2006).
- [12] A.C. Aguilar, A.A. Natale, and P.S. Rodrigues da Silva, Phys. Rev. Lett. **90**, 152001 (2003).
- [13] F.D.R. Bonnet *et al.*, Phys. Rev. D **64**, 034501 (2001); A. Cucchieri, T. Mendes, and A. Taurines, Phys. Rev. D **67**, 091502(R) (2003); P.O. Bowman *et al.*, Phys. Rev. D **70**, 034509 (2004); A. Sternbeck, E.-M. Ilgenfritz, M. Muller-Preussker, and A. Schiller, Phys. Rev. D **72**, 014507 (2005); A. Sternbeck, E.-M. Ilgenfritz, and M. Muller-Preussker, **73**, 014502 (2006); Ph. Boucaud *et al.*, JHEP **0606**, 001 (2006); P.O. Bowman *et al.*, hep-lat/0703022.
- [14] A.C. Aguilar, A. Mihara, and A.A. Natale, Phys. Rev. D **65**, 054011 (2002); Int. J. Mod. Phys. A **19**, 249 (2004).
- [15] M.B. Gay Ducati, F. Halzen, and A.A. Natale, Phys. Rev. D **48**, 2324 (1993); F. Halzen, G. Krein, and A.A. Natale, Phys. Rev. D **47**, 295 (1993).
- [16] E.G.S. Luna, Phys. Lett. B **641**, 171 (2006).
- [17] E.G.S. Luna and A.A. Natale, Phys. Rev. D **73**, 074019 (2006).
- [18] E.G.S. Luna, Braz. J. Phys. **37**, 84 (2007); A.A. Natale, Braz. J. Phys. **37**, 306 (2007).
- [19] V.N. Gribov and L.N. Lipatov, Sov. J. Nucl. Phys. **15**, 438 (1972); G. Altarelli and G. Parisi, Nucl. Phys. B **126**, 298 (1977); Yu.L. Dokshitzer, Sov. Phys. JETP **46**, 641 (1977).
- [20] H. Pagels and S. Stokar, Phys. Rev. D **20**, 2947 (1979).
- [21] S.J. Brodsky and G. Farrar, Phys. Rev. Lett. **31**, 1153 (1973).
- [22] J.M. Cornwall and A. Soni, Phys. Lett. B **120**, 431 (1983).
- [23] P.D.B. Collins, *Regge Theory and High Energy Physics* (Cambridge University Press, Cambridge, 1977); S. Donnachie, G. Dosch, P. Landshoff, O. Nachtmann, *Pomeron Physics and QCD* (Cambridge University Press, Cambridge, 2002); V. Barone, E. Predazzi, *High-Energy*

Particle Diffraction (Springer-Verlag, Berlin, 2002).

- [24] E.G.S. Luna and M.J. Menon, Phys. Lett. B **565**, 123 (2003).
- [25] E.G.S. Luna, M.J. Menon, and J. Montanha, Nucl. Phys. A **745**, 104 (2004).
- [26] A. Donnachie and P.V. Landshoff, Phys. Lett. B **437**, 408 (1998).
- [27] Ya.Ya. Balitsky and L.N. Lipatov, Sov. J. Nucl. Phys. **28**, 822 (1977); E.A. Kuraev, L.N. Lipatov, and V. Fadin, Soviet Physics JETP **45**, 199 (1977).
- [28] J. Kwieciński, A.D. Martin, and P.J. Sutton, Phys. Lett. B **264**, 199 (1991); Phys. Rev. D **44**, 2640 (1991); **46**, 921 (1992).
- [29] J.R. Forshaw and P.N. Harriman, Phys. Rev. D **46**, 3778 (1992).
- [30] D.A. Ross, J. Phys. G **15**, 1175 (1989).
- [31] A. Donnachie and P.V. Landshoff, Phys. Lett. B **296**, 227 (1992).
- [32] A. Donnachie and P.V. Landshoff, Nucl. Phys. B **231**, 189 (1983).
- [33] R.F. Ávila, E.G.S. Luna, and M.J. Menon, Phys. Rev. D **67**, 054020 (2003).
- [34] F. Abe *et al.*, Phys. Rev. D **50**, 5550 (1993).
- [35] N.A. Amos *et al.*, Phys. Rev. Lett. **68**, 2433 (1992).
- [36] C. Avila *et al.*, Phys. Lett. B **445**, 419 (1999).
- [37] J.R. Cudell, A. Donnachie, and P.V. Landshoff, Nucl. Phys. B **322**, 55 (1989).
- [38] A.D. Martin, R.G. Roberts, W.J. Stirling, and R.S. Thorne, Phys. Lett. B **531**, 216 (2002).
- [39] J. Pumplin *et al.*, JHEP **0207**, 012 (2002); D. Stump *et al.*, *ibid* **0310**, 046 (2003).
- [40] H.R. Christiansen and J. Magnin, Phys. Lett. B **445**, 8 (1998); Phys. Rev. D **63**, 014001 (2000).
- [41] J. Alwall and G. Ingelman, Phys. Rev. D **70**, 111505(R) (2004); Phys. Rev. D **71**, 094015 (2005).
- [42] J. Alwall and G. Ingelman, Phys. Lett. B **596**, 77 (2004).
- [43] A.D. Martin, R.G. Roberts, W.J. Stirling, and R.S. Thorne, Eur. Phys. J. C **4**, 463 (1998).
- [44] P.V. Landshoff and O. Nachtmann, Z. Phys. C **35**, 405 (1987).
- [45] A.I. Shoshi, F.D. Steffen, and H.J. Pirner, Nucl. Phys. A **709**, 131 (2002).
- [46] A.I. Shoshi, F.D. Steffen, H.G. Dosch, and H.J. Pirner, Phys. Rev. D **66**, 094019 (2002).
- [47] V.A. Khoze, A.D. Martin, and M.G. Ryskin, Eur. Phys. J. C **18**, 167 (2000).

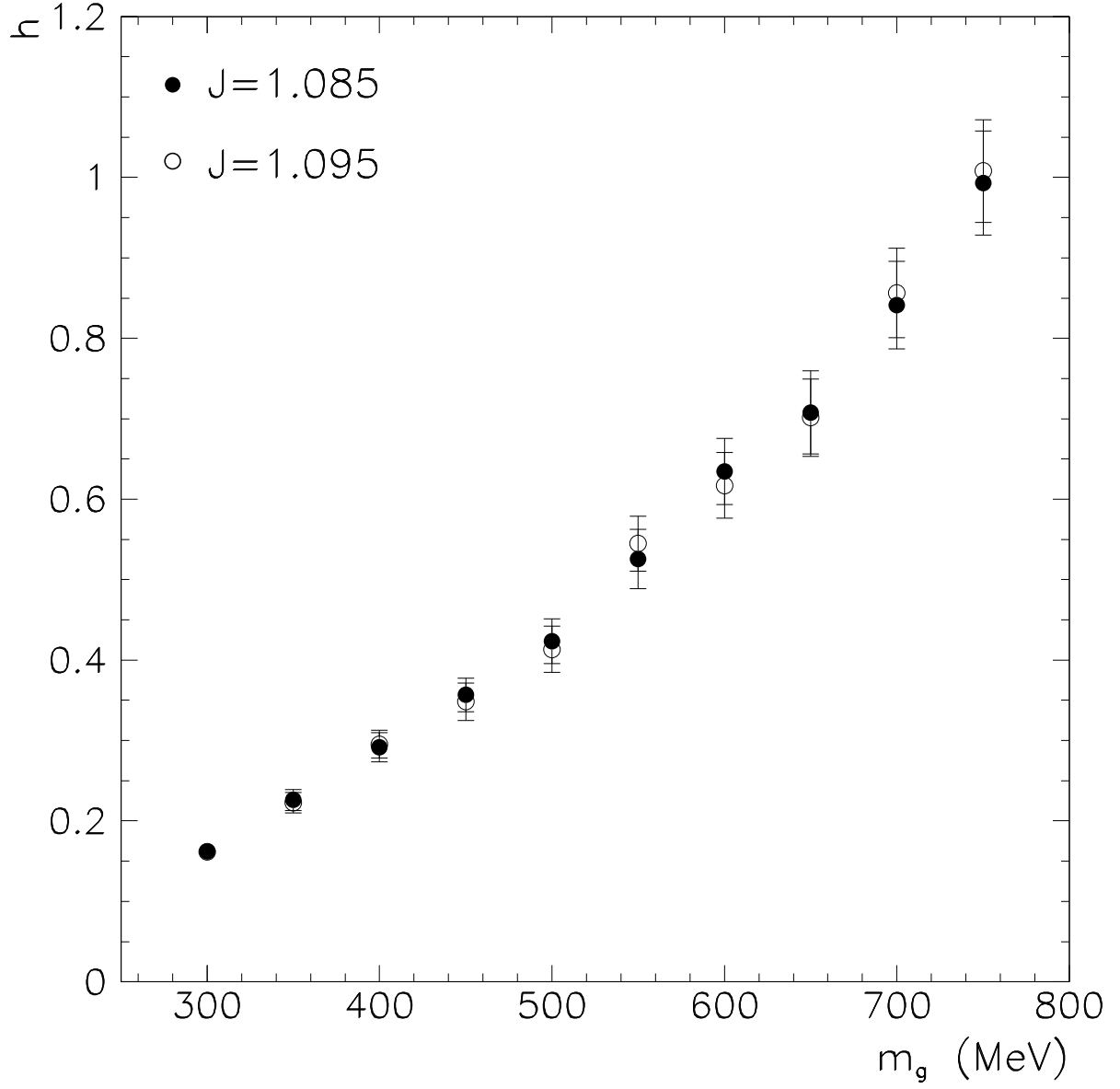


FIG. 1: The factor h as a function of the gluon dynamical mass m_g determined by means of the DGM model.

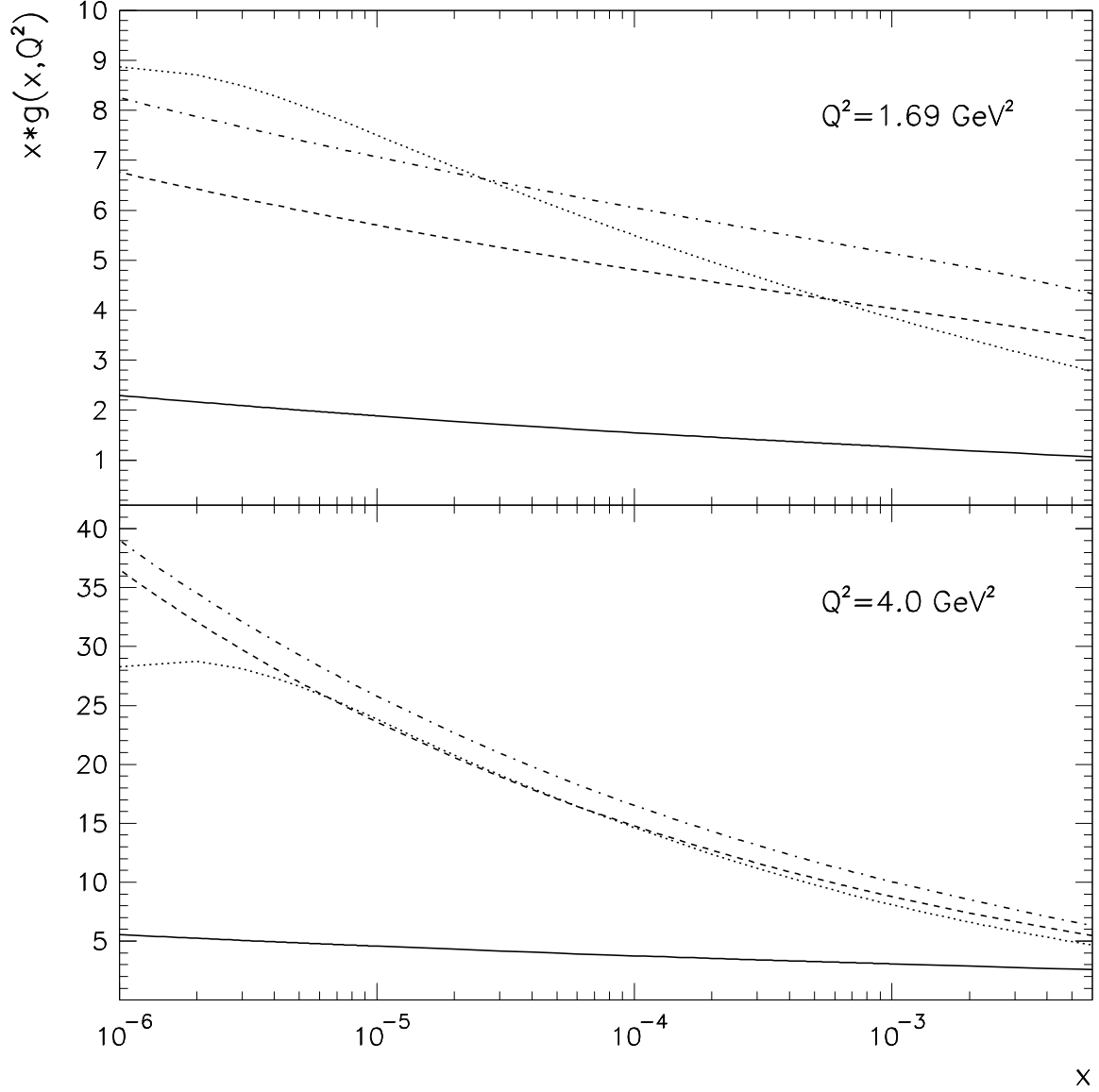


FIG. 2: The gluon distributions at $Q^2 = 1.69$ and 4.0 GeV^2 from the DGM model (solid curves). The dotted, dashed and dotted-dashed curves are the distributions corresponding to the MRST, CTEQ6L1 and CTEQ6L gluon sets, respectively.

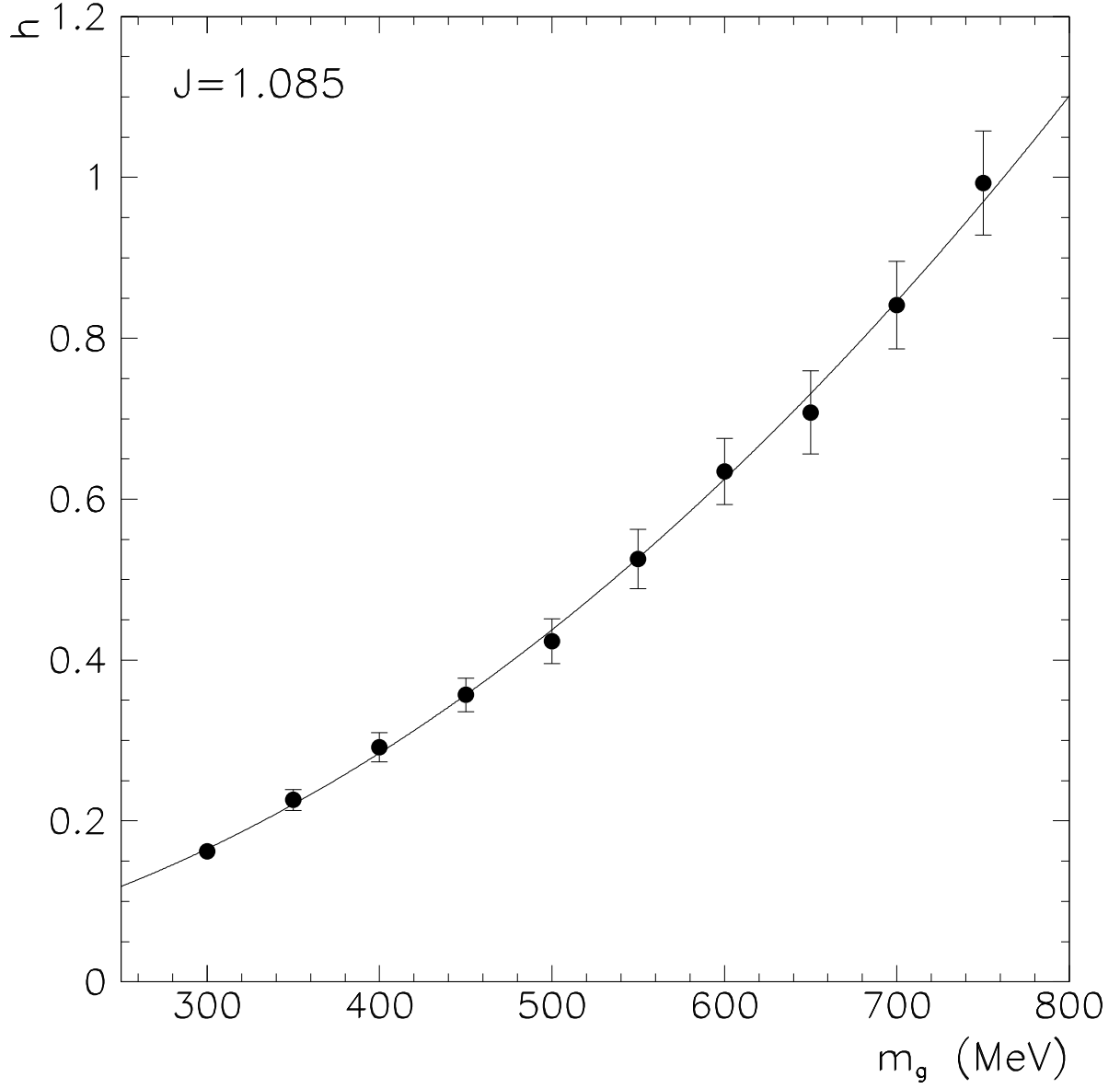


FIG. 3: The factor h as a function of the gluon dynamical mass m_g . The solid curve is obtained through the function $h(Q^2) = A + BQ^2$, with $A = 0.121 \times 10^{-1}$ and $B = 0.170 \times 10^{-5} \text{ MeV}^{-2}$.